

Supporting Information

Amino Acid-Derived Cu(II)-Coordinated Supramolecular Hydrogel with Tunable Mechanics, Self-Healing, and Underwater Adhesion

Nishikanta Singh,^[a] Koushik Mahata,^[b] Durgesh Kumar Sinha,^[a] and Sanjib Banerjee*^[a]

^aDepartment of Chemistry, Indian Institute of Technology Bhilai, Durg 491002, Chhattisgarh, India

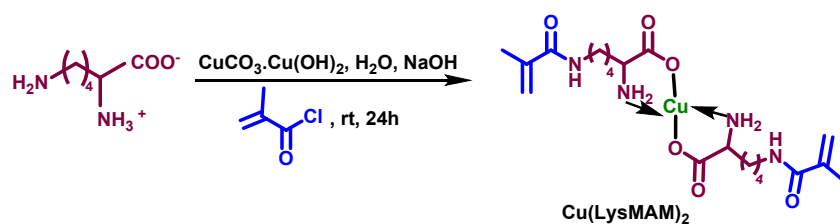
^bDepartment of Materials Science and Metallurgical Engineering, Indian Institute of Technology Bhilai, Durg 491002, Chhattisgarh, India

*Corresponding Author

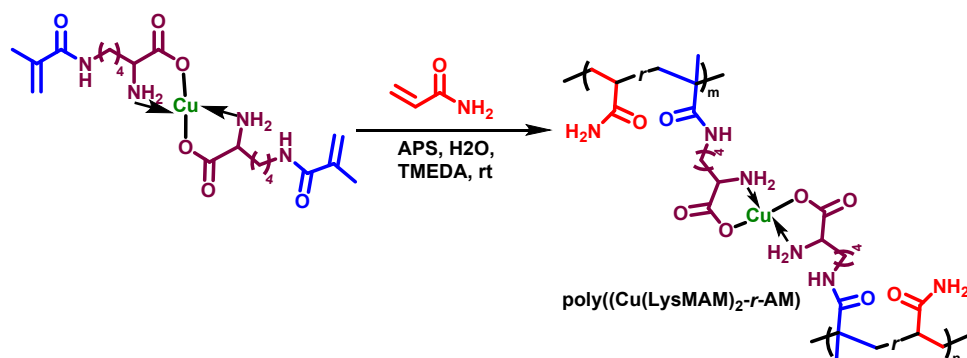
E-mail: sanjib.banerjee@iitbhilai.ac.in

SB. Supporting Tables, Schemes, and Figures	S3-S9
Scheme S1. Synthesis of Cu(LysMAM) ₂ crosslinker.	S3
Scheme S2. Synthesis of poly(Cu(LysMAM) _{2-r} -AM) hydrogel.	S3
Scheme S3. Deprotection of poly(Cu(LysMAM) _{2-r} -AM) to poly(LysMAM- <i>r</i> -AM).	S3
Figure S1. ¹ H NMR spectrum of Cu(LysMAM) ₂ crosslinker in D ₂ O.	S4
Figure S2. ATR-IR spectra of (a) L-lysine and Cu(LysMAM) ₂ . (b) poly(Cu(LysMAM) _{2-r} -AM) hydrogel, Cu(LysMAM) ₂ and AM	S4
Figure S3. EDS mapping of Cu(LysMAM) ₂ .	S5
Figure S4. Reversibility of poly(Cu(LysMAM) _{2-r} -AM) hydrogel.	S5
Figure S5. Rheology of the metallo-supramolecular hydrogel poly(Cu(LysMAM) _{2-r} -AM).	S6
Figure S6. Swelling study of the hydrogel in different solvents, i.e. deionized water, DMSO, ethanol, and toluene.	S6
Figure S7. Lap-shear test data of poly(Cu(LysMAM) _{2-r} -AM) hydrogel adhesive on glass surfaces before and after swelling in water for 24 h.	S7
Table S1. Correlations and participants' information on flat foot detection.	S7
Figure S8. Represents the effect of pressure on the resistance of poly(Cu(LysMAM) _{2-r} -AM) hydrogel.	S8
Figure S9. Represents the reversibility of poly(Cu(LysMAM) _{2-r} -AM) hydrogel in flat foot setup.	S8
Table S2. Comparison with other reported metal-ion and supramolecular hydrogels.	S9
References	S10

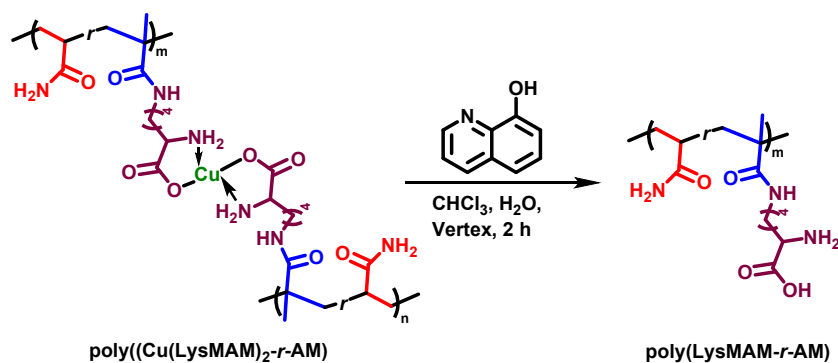
B. Supporting Tables, Schemes, and Figures



Scheme S1. Synthesis of Cu(LysMAM)_2 crosslinker.



Scheme S2. Synthesis of $\text{poly}(\text{Cu(LysMAM)}_2\text{-}r\text{-AM})$ hydrogel.



Scheme S3. Deprotection of $\text{poly}(\text{Cu(LysMAM)}_2\text{-}r\text{-AM})$ to $\text{poly(LysMAM-}r\text{-AM)}$.

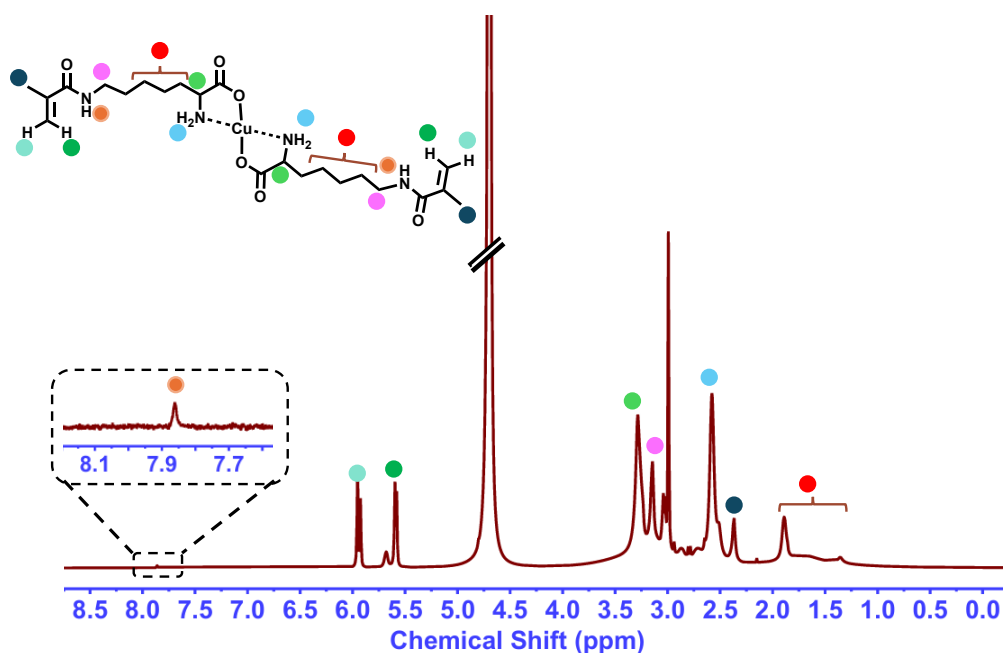


Figure S1. ^1H NMR spectrum of $\text{Cu}(\text{LysMAM})_2$ crosslinker in D_2O .

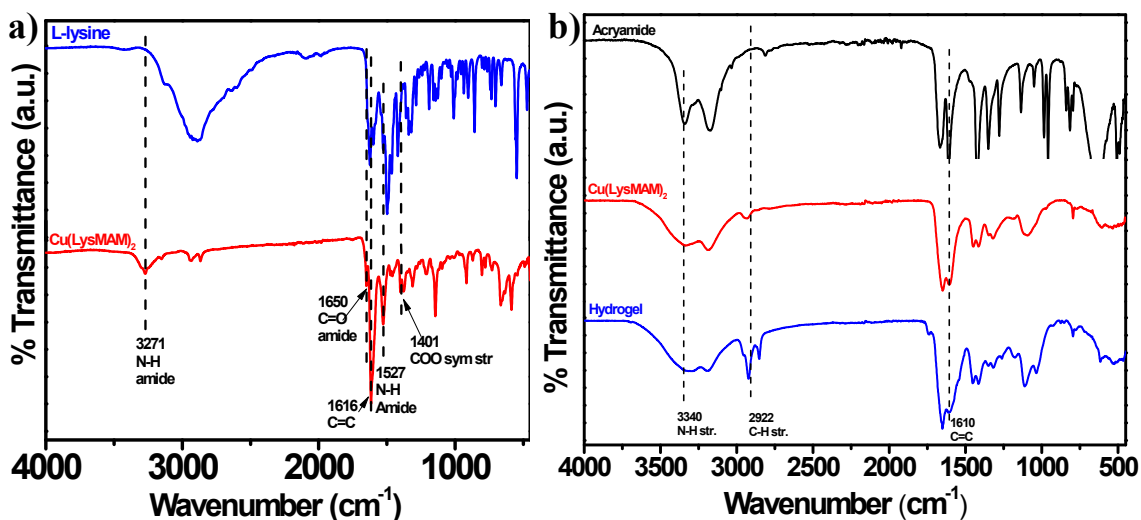


Figure S2. ATR-IR spectra of (a) L-lysine and $\text{Cu}(\text{LysMAM})_2$. (b) poly($\text{Cu}(\text{LysMAM})_2$ -*r*-AM) hydrogel, $\text{Cu}(\text{LysMAM})_2$ and AM.

ATR-IR spectroscopy (Figure S2(a)) shows the characteristic stretching of N-H of amide at 3271 cm^{-1} , C=O of amide at 1650 cm^{-1} , N-H sym stretching at 1527 cm^{-1} , 1640 cm^{-1} corresponds to C=C of $\text{Cu}(\text{LysMAM})_2$. (Figure S2(b)) shows the ATR-IR spectroscopy of poly($\text{Cu}(\text{LysMAM})_2$ -*r*-AM) hydrogel at $3400\text{--}3000\text{ cm}^{-1}$, $\nu\text{N-H}$ (amine, amide); 2925 cm^{-1} , $\nu\text{C-H}$ (vinyl); 1530 cm^{-1} , absence of 1610 cm^{-1} , $\nu\text{C=C}$; confirms the successful polymerization of AM and $\text{Cu}(\text{LysMAM})_2$.

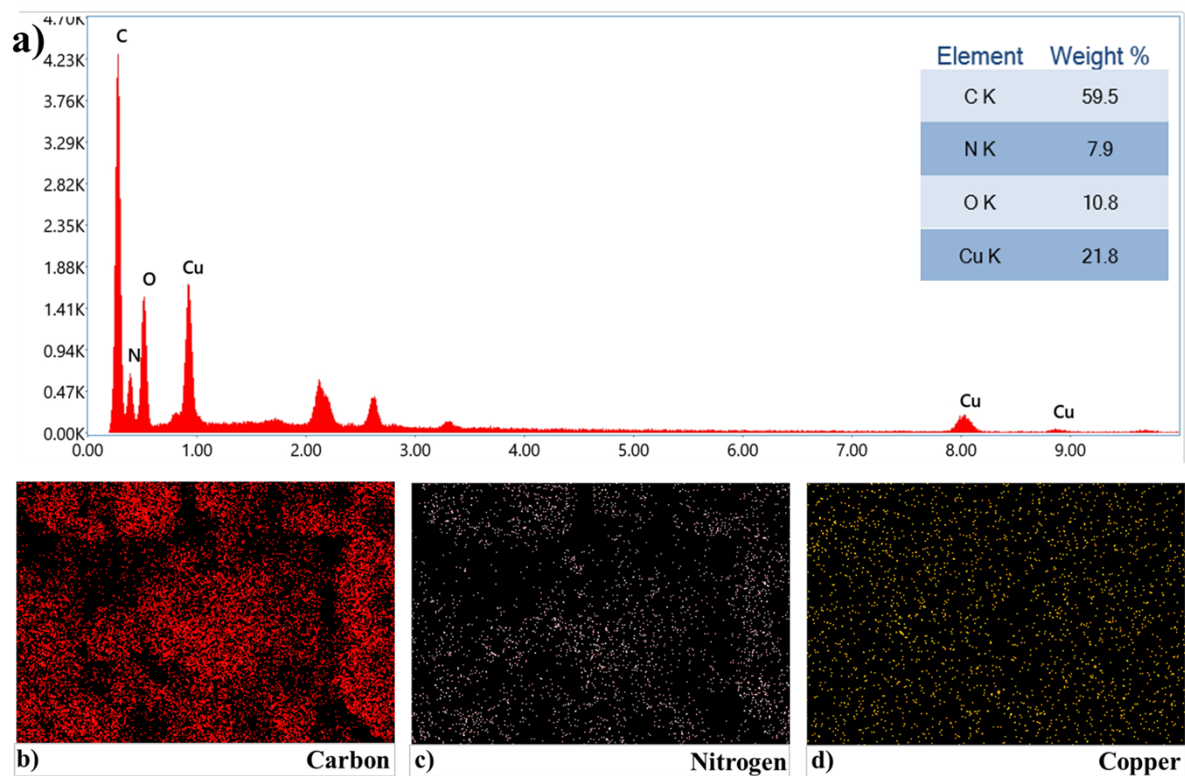


Figure S3. EDS mapping of $\text{Cu}(\text{LysMAM})_2$.

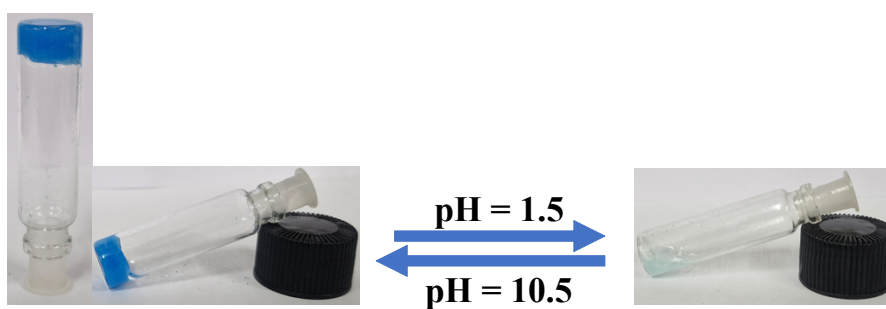


Figure S4. Represents the reversibility of $\text{poly}(\text{Cu}(\text{LysMAM})_2\text{-}r\text{-AM})$ hydrogel. Adding NaOH binds the polymer with metal ions to form a hydrogel material, which can be reversed by adding HCl to the hydrogel.

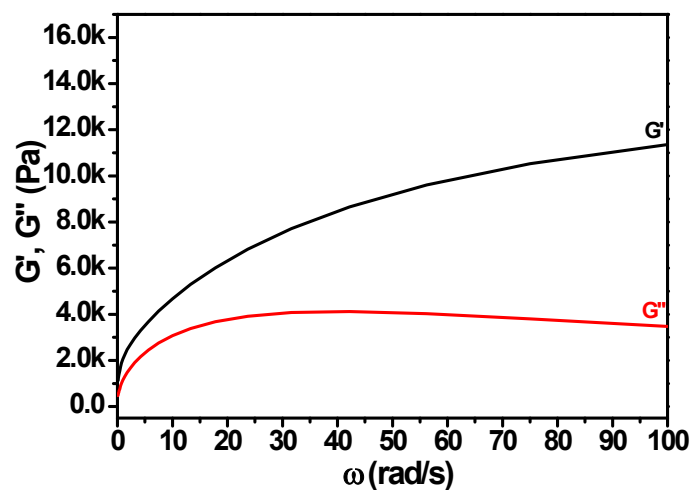


Figure S5. Rheology of the metallo-supramolecular hydrogel poly(Cu(LysMAM)₂-*r*-AM).

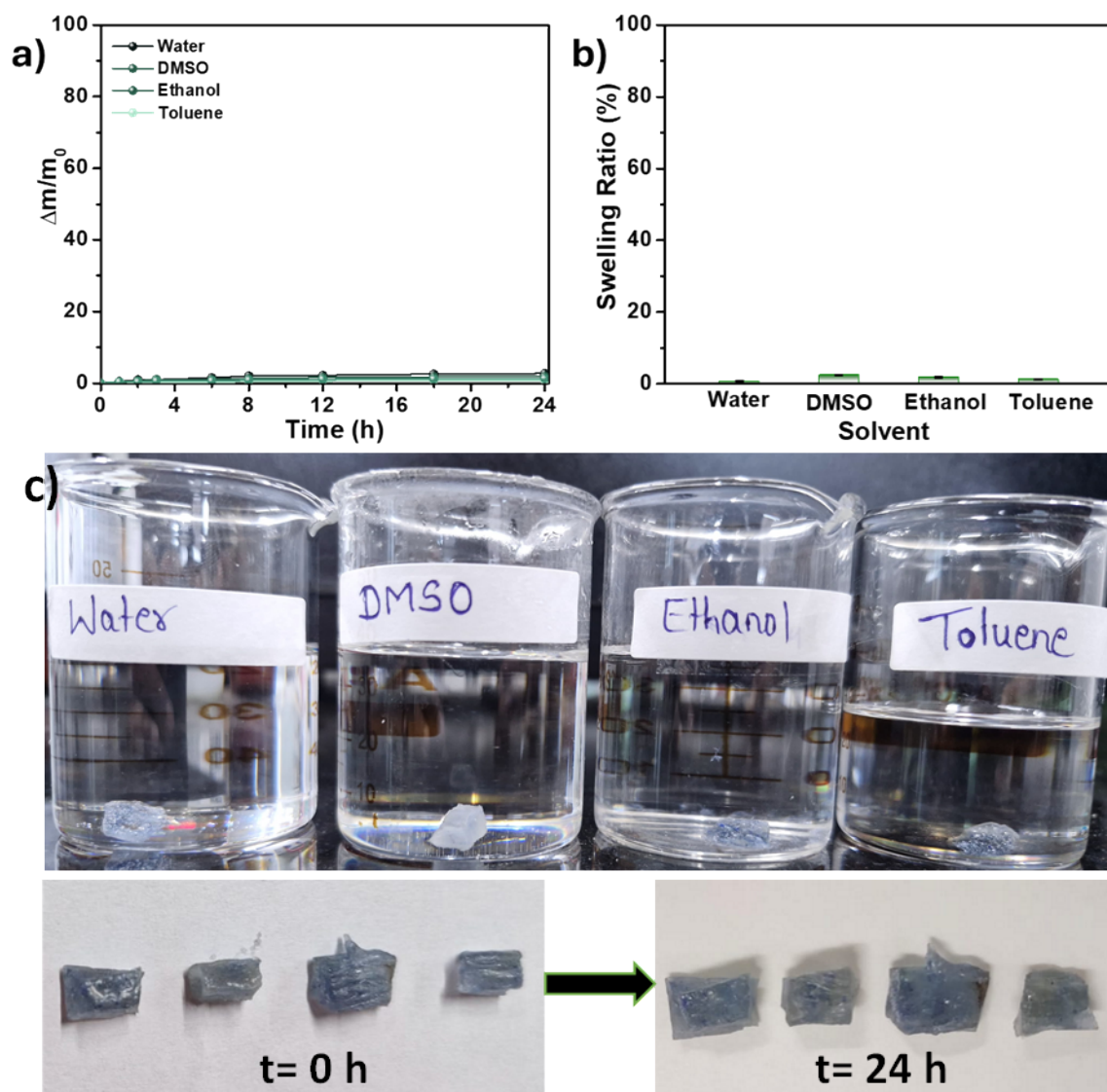


Figure S6. Swelling study of the hydrogel in different solvents, i.e. deionized water, DMSO, ethanol, and toluene; (a) time-dependent swelling behavior ($\Delta m/m_0$) of poly(Cu(LysMAM)₂-*r*-AM) gels, (b) corresponding equilibrium swelling ratios (%), (c) Images of hydrogels illustrating their swelling in various solvents, along with a comparison of their appearance before and after swelling.

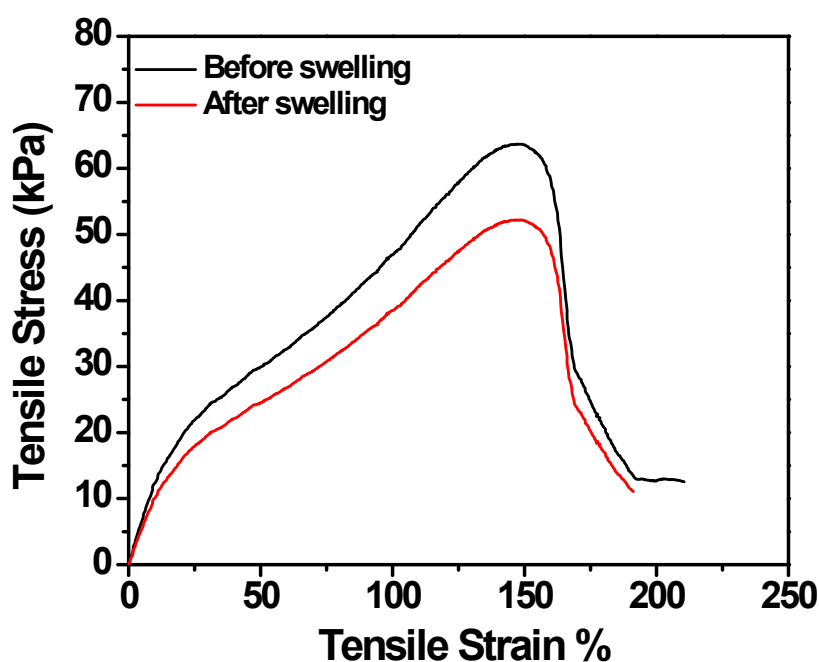


Figure S7. Lap-shear test data of poly(Cu(LysMAM)₂-*r*-AM) hydrogel adhesive on glass surfaces before and after swelling in water for 24 h.

Table S1. Correlations and participants' information on flat foot detection

Gender	No. of participants	Average age	Average Shoe size	Average body weight
Female	22	22-28	38	48 kg
Male	25	22-28	42	65 kg

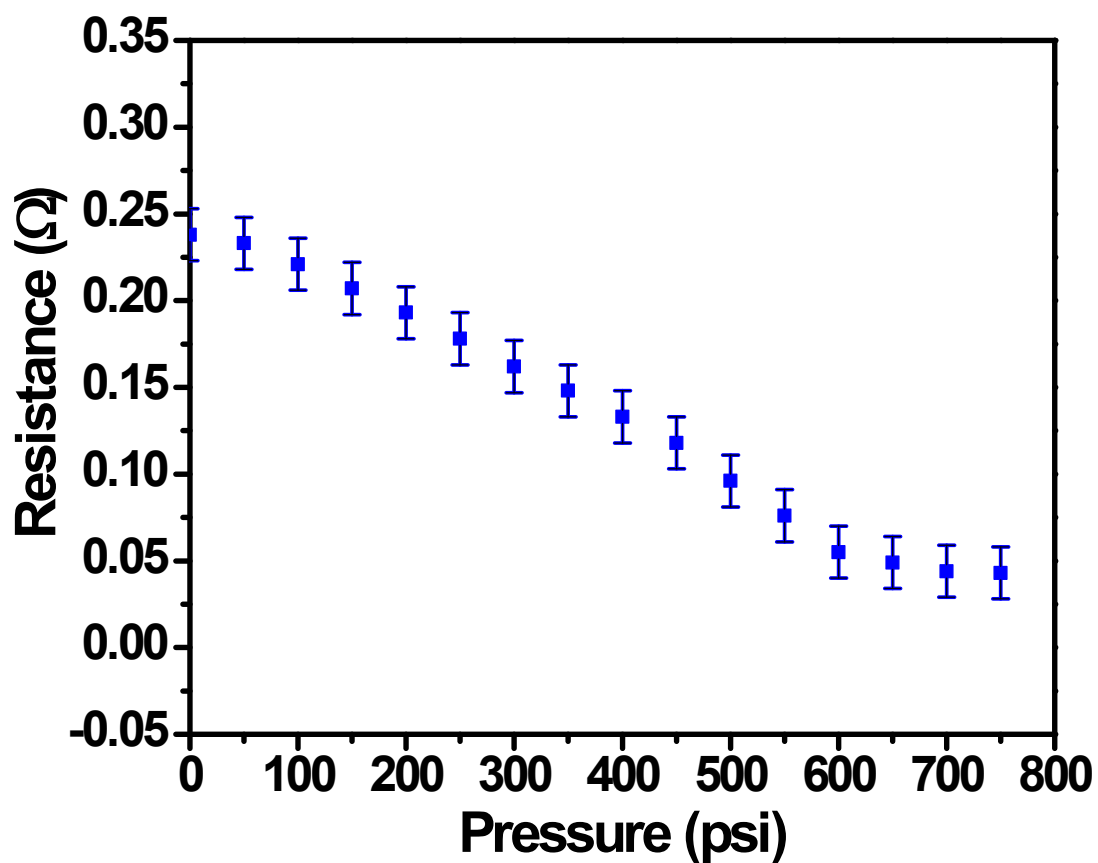


Figure S8. Represents the effect of pressure on the resistance of poly(Cu(LysMAM)₂-*r*-AM) hydrogel.

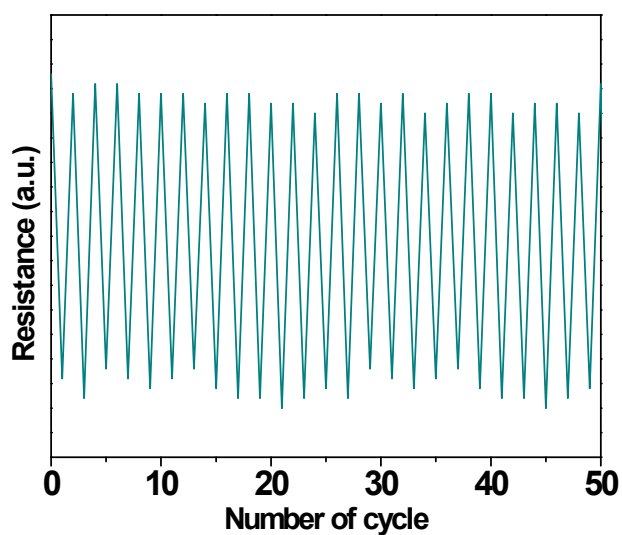


Figure S9. Represents the reversibility of poly(Cu(LysMAM)₂-*r*-AM) hydrogel in flat foot setup.

Table S2. Comparison with other reported metal-ion and supramolecular hydrogels.

Hydrogel System	Tensile Strength	Self-Healing Efficiency	Adhesion	Reference
This Work (poly(Cu(LysMAM) ₂ - <i>r</i> -AM))	140 kPa	~92% in 1 h	Good underwater adhesion	This Work
Zn(II) Salphen metallogel complexes	~100 Pa	No Self-healing	No adhesion	1
peptide/Zn ²⁺ hydrogel	~80 Pa	No Self-healing	No adhesion	2
TA@CNC/PVA/gel hydrogels	25.54 kPa	93 % in 1 h	The strong adhesion to wood, paper, copper sheets, glass, and surface.	3
Cu(II)–Inosine Supramolecular Gel	10 kPa	3 h	No adhesion	4
DCMC/CS/PAA Polysaccharide-Composite Hydrogel	90 kPa	93% in 24 h	Self-adhesion	5
CNF–Al ³⁺ –Xylan Nanocomposite	31.1 kPa	95% in 2 h	Yes	6
Chitosan–HA–Al ³⁺ Hydrogel	379.5 kPa	~87%	Not specified	7
P(AM-HisMA)-Fe ³⁺ –Hydrogel	89 kPa	>84% in 5 min	Porcine skin	8
3D-printed PVC/DBA Hydrogel	26.4 kPa	Not reported	Not reported	9

Ru(II)-metallogel	1.4 kPa	No Self-healing	No adhesion	10
Ag ⁺ and Fe ³⁺ -metallogels	10 kPa	No Self-healing	No adhesion	11
Fe ³⁺ -P(AAm-co-AAc) Hydrogel	7 kPa	Yes	Not reported	12

Reference

1. Stühler, M. R.; Makki, H.; Silbernagl, D.; Dimde, M.; Ludwig, K.; Tegner, B. E.; Greve, C.; Rausch, K.; Herzig, E. M.; Köhler, A., Flexibility and Dynamicity Enhances and Controls Supramolecular Self-Assembly of Zinc (II) Metallogels. *Adv. Funct. Mater.* **2025**, 2507793.
2. Adole, V. V.; Wang, Z.; Tang, Y.; Mishra, G.; Sahu, I.; Wei, G.; Chakraborty, P., Histidine Containing Minimalistic-Peptide-Based Nanostructured Hydrogel for Multiple Enzyme-Mimicking Catalytic Activities. *Small* **2025**, 21 (51), e11661.
3. Gu, R.; Chen, W.; Zou, Y.; Yang, T.; Liu, Z.; Yu, N.; Huang, J.; Gan, L., Cellulose nanocrystal-modified hydrogel wearable sensor with self-healing function from dynamic bond and controllable dual hydrogen-bond crosslinking. *Carbohydr. Polym.* **2025**, 363, 123760.
4. Singh, S.; Rohilla, K.; Verma, N.; Sharma, B., Cu(II)-Inosine Supramolecular Gel with Nanofibrous Morphology as Laccase and Peroxidase Mimic for Optical Sensing Applications. *ACS Appl. Nano Mater.* **2025**, 8 (32), 15953-15965.
5. Ling, Q.; Liu, W.; Liu, J.; Zhao, L.; Ren, Z.; Gu, H., Highly Sensitive and Robust Polysaccharide-Based Composite Hydrogel Sensor Integrated with Underwater Repeatable Self-Adhesion and Rapid Self-Healing for Human Motion Detection. *ACS Appl. Mater. Interfaces* **2022**, 14 (21), 24741-24754.
6. Liu, X.; Chang, M.; Zhang, H.; Ren, J., Rapid self-healing and adhesion nanocomposite physical hydrogels based on dynamic coordination bond. *Polym Adv Technol.* **2022**, 33 (12), 4174-4185.

7. Zhang, Q.; Li, C.; Du, X.; Zhong, H.; He, Z.; Hong, P.; Li, Y.; Jing, Z., High strength, tough and self-healing chitosan-based nanocomposite hydrogels based on the synergistic effects of hydrogen bond and coordination bond. *J. Polym. Res.* **2022**, *29* (8), 335.
8. Zhang, H.; He, J.; Qu, J., Metal-coordinated amino acid hydrogels with ultra-stretchability, adhesion, and self-healing properties for wound healing. *Eur. Polym. J.* **2022**, *179*, 111548.
9. Wang, Z.; Wang, Y.; Wang, Z.; He, Q.; Li, C.; Cai, S., 3D Printing of Electrically Responsive PVC Gel Actuators. *ACS Appl. Mater. Interfaces* **2021**, *13* (20), 24164-24172.
10. Malviya, N.; Sonkar, C.; Ganguly, R.; Bhattacharjee, D.; Bhabak, K. P.; Mukhopadhyay, S., Novel Approach to Generate a Self-Deliverable Ru(II)-Based Anticancer Agent in the Self-Reacting Confined Gel Space. *ACS Appl. Mater. Interfaces* **2019**, *11* (50), 47606-47618.
11. Panja, A.; Ghosh, K., Cholesterol-based diazine derivative: selective sensing of Ag⁺ and Fe³⁺ ions through gelation and the performance of metallo gels in dye and picric acid adsorption from water. *Mater. Chem. Front.* **2018**, *2* (12), 2286-2296.
12. Zheng, S. Y.; Ding, H.; Qian, J.; Yin, J.; Wu, Z. L.; Song, Y.; Zheng, Q., Metal-Coordination Complexes Mediated Physical Hydrogels with High Toughness, Stick-Slip Tearing Behavior, and Good Processability. *Macromolecules* **2016**, *49* (24), 9637-9646.